

# Validation of a novel open source software suite against an extensive data set of automotive aerodynamics test cases

**A Lock, T Johansen**  
Auto Research Center LLC, USA

**P Geremia**  
Engys Srl, Italy

**E de Villiers**  
Engys Ltd, UK

## Abstract

This paper presents the results of a multi-year development and validation exercise for a novel open source Computational Fluid Dynamics (CFD) software suite. The software makes use of an advanced meshing methodology and a Delayed Detached Eddy Simulation (DDES) flow solver to accurately predict the aerodynamic forces on a range of different vehicle shapes. In addition a graphical user interface (GUI) has been created that automates most of the set-up of the case and has embedded best practices, dependent on vehicle shape, to ensure accurate and repeatable results for users in an industrial development process.

As well as improving the accuracy of the DDES simulations through use of meshing and solver best practices, significant effort has taken place to improve the solution times providing benefit for single CFD simulations, but also significantly reducing the turnaround time of Design Of Experiment (DOE) style optimization projects.

The validation of the software suite has been extensive, with over 100 different vehicle configurations compared to wind tunnel data. The vehicle shapes used were diverse, covering sedans, hatchbacks, estates and SUVs, motorsport applications, as well as both light and heavy duty trucks. In addition to different vehicle shapes a wide range of experimental configurations were evaluated including different ground simulation techniques, yaw angles, ride heights and test speeds. Although the focus was on improving absolute accuracy, deltas for part changes were also checked for directionality and magnitude.

Finally the paper will also briefly discuss future prospects for the software suite.

## Introduction

The Elements Software Suite is a new CFD solution resulting from a joint venture, Streamline Solutions, between the Auto Research Center, an automotive consultancy based in Indianapolis, and Engys, a software development company

specializing in open source CFD and optimisation, based in London.

The objective of the project was to develop a set of best practice methodologies that not only ensured accurate results from the suite but also a robust process that delivered significant benefits in turnaround times for transient CFD simulations. In order to achieve this a large data set was created of wind tunnel results from the Auto Research Center model-scale, moving ground wind tunnel, as well as numerous full-scale wind tunnels from around the world.

The best practice methodologies were also characterized by vehicle shape (including hatchback, SUV; coupe, truck, etc.), in order to allow users in an industrial environment to use a consistent, and hence repeatable, approach. See Figure 1.

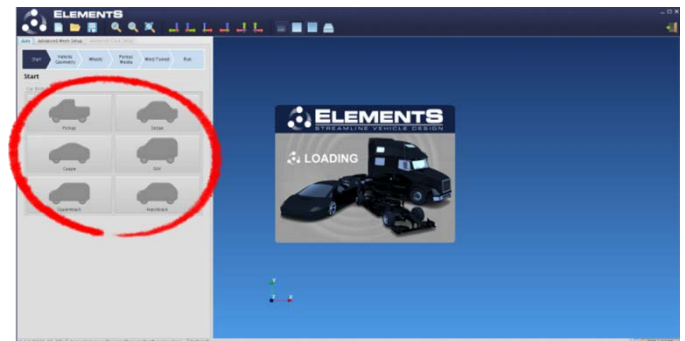


Figure 1. Screenshot of the GUI, with vehicle shape choices highlighted.

## Methodology

### Meshing Strategy

For most of the configurations simulated the far-field is scaled based on vehicle dimensions in order to minimize the effects of blockage, whilst also ensuring that the inlet and outlet are far enough away from the vehicle to minimize unwanted numerical

interactions. This procedure is based on the recommendations of SAE Standard J2966\_201309 [1], and results in a domain that is 10 vehicle widths wide, 6 vehicle heights high and 20 vehicle lengths long. See Figure 2.

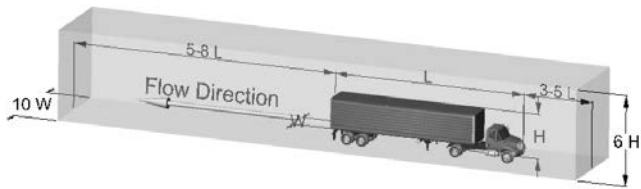


Figure 2. Overview of the domain sizing.

For some configurations, however, it was found that a better correlation could be achieved if the physical wind tunnel was represented in the computational domain, thus capturing any pressure gradient effects. An example of this approach is shown in Figure 3.

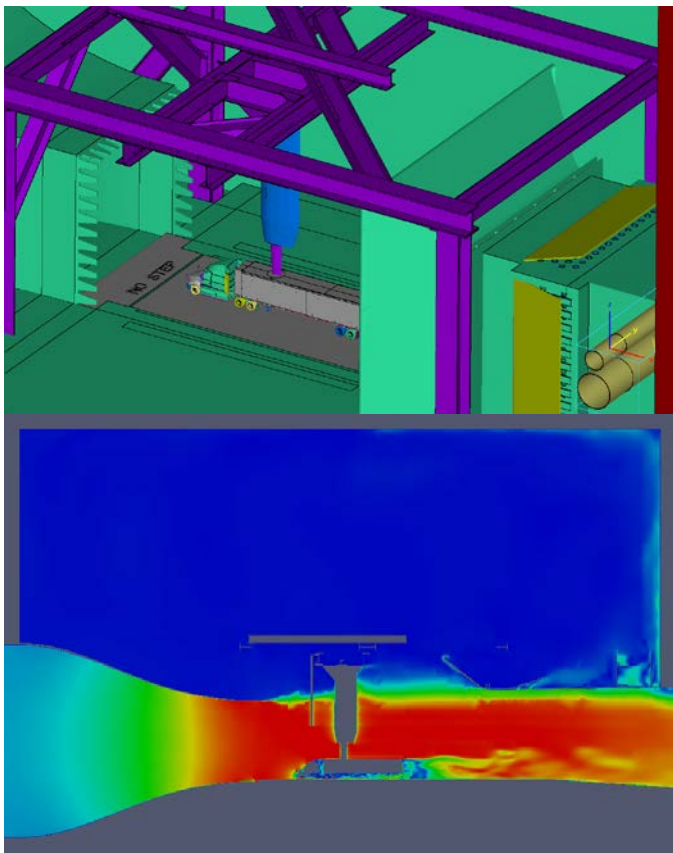


Figure 3. Example of use of physical wind tunnel geometry.

A hex-dominant mesh generator was then employed to create the computational grid. The mesher incorporates crack and hole detection algorithms to cope with 'dirty' CAD data. A base block mesh is then refined using a number of techniques, summarized below:

1. Refinement boxes – the default method for defining nested regions of additional refinement, defined by 2 corners. Typically 5 of these are used.

2. Refinement primitives – basic shapes such as a box, cylinder, sphere, plane, etc.
3. STL geometry based refinement – custom shapes used for wake refinement.
4. Distance refinement – additional refinement based on proximity to a surface. Up to 3 levels of distance refinement are used to increase mesh density close to regions with high gradients.
5. Surface curvature based refinement – refinement based on surface curvature, includes feature edge snapping.

A typical mesh generated for an estate back model is shown in Figure 4.

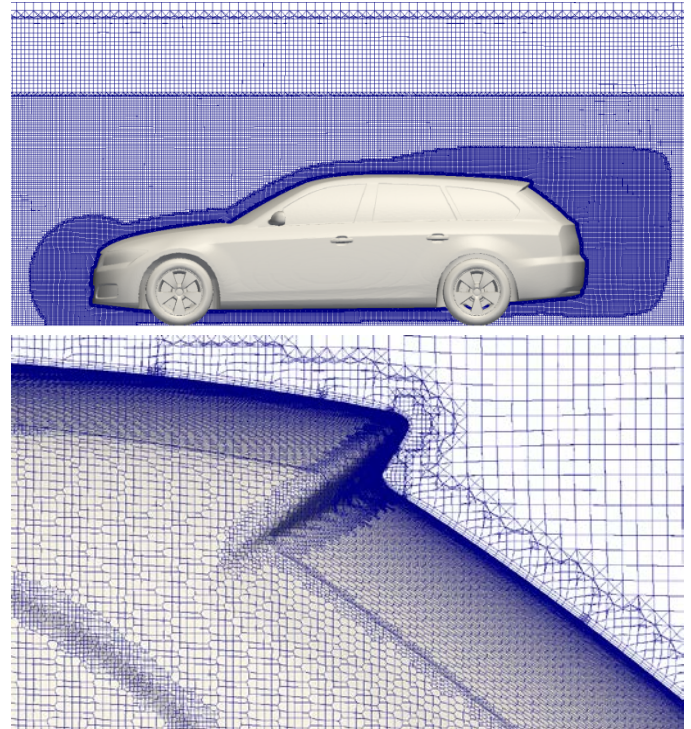


Figure 4. Example of refinement boxes, STL refinement and distance refinement approaches used for a coupe body shape.

In Figure 4 notice how bespoke wake zone refinement is automatically applied to accurately resolve the separated area at the rear of the car. Similarly, for a correct prediction of the stagnation region on the front grill a cylinder shape refinement box is automatically added based on vehicle dimensions and position in the wind tunnel.

Initially meshes were created without prism layers due to their computational cost to both the meshing and solving processes. This gave drag accuracies that met expectations for most body shapes, but failed for certain square-back body styles, and also failed to give the target accuracy for lift. Subsequently 3 prism layers have been applied, which gives the required accuracies. A significant amount of development effort has gone into minimizing the computational cost of prism layers.

## Solution Method

The solution methodology used in this work is based on Detached Eddy Simulation (DES) modelling [2] [3]. The DES approach consists of a direct simulation of the larger energy-containing structures, while the finer scales are modelled, like in the LES approach, and in addition to solve the RANS equations in the near-wall regions, where a complete resolution of the energy-containing turbulence structures would require fine grids and small time-step increments, not affordable for complex applications. The major advantage of DES with respect to other unsteady approaches like URANS is that the resolved turbulence depends on mesh density. The DES approach relies on a modified turbulence model that can operate either as a standard RANS model in the near-wall regions or as a sub-grid eddy viscosity model in the rest of the domain. The Smagorinsky-type sub-grid scale is used in wake and separate regions away from surfaces (LES regions), while a Spalart-Allmaras model is employed in the attached boundary layer (RANS regions). To increase robustness and stability of the solution, a specific blending function for the advection schemes of the momentum equation based on local Courant number and near-wall distance was implemented [4].

DDES is a modification of the Detached Eddy Simulation (DES) model to improve its performance in thick boundary layers and shallow separation regions. According to Spalart et al. [5], for "ambiguous" grids DES shows premature transition between RANS and LES mode leading to artificial separation also known as Grid Induced Separation (GIS).

As with any transient simulation a compromise typically has to be reached between using a large timestep to reduce computational time, and a small timestep to give better accuracy. In Elements this is solved by using a coarse time step ( $\sim 5e-3$  seconds) to initialize the solution followed by a smaller time step ( $\sim 2e-4$  seconds) to accurately resolve intrinsic flow instabilities. Both values are automatically calculated, based on vehicle length and free-stream velocity. Significant development effort had to take place for both mesh quality and solution strategies in order for the large timestep initialization phase to run reliably.

Total 'real time' simulated varies from 1 second for model scale cars to 5 seconds for trucks. These numbers are designed to allow for a full pass of the fluid domain during the initialization phase, and 5 passes of the vehicle during the fine timestep phase.

Heat exchangers are treated as porous media using the Darcy Forchheimer Law, based on measured pressure versus velocity curves. Cooling fans are modelled using a Multiple Reference Frame (MRF) approximation to take into account the effect of the rotation on the cooling mass flow. Finally, wheels are treated either as rotating walls, or more recently as sliding mesh regions.

Automated post-processing routines are employed to create contour plots of velocity, pressure (both static and total), near-wall velocity, and other relevant quantities. In addition force, and moment, development graphs were made available for quick assessment of the vehicle aerodynamic performance. Some examples of these are shown in Figure 5.

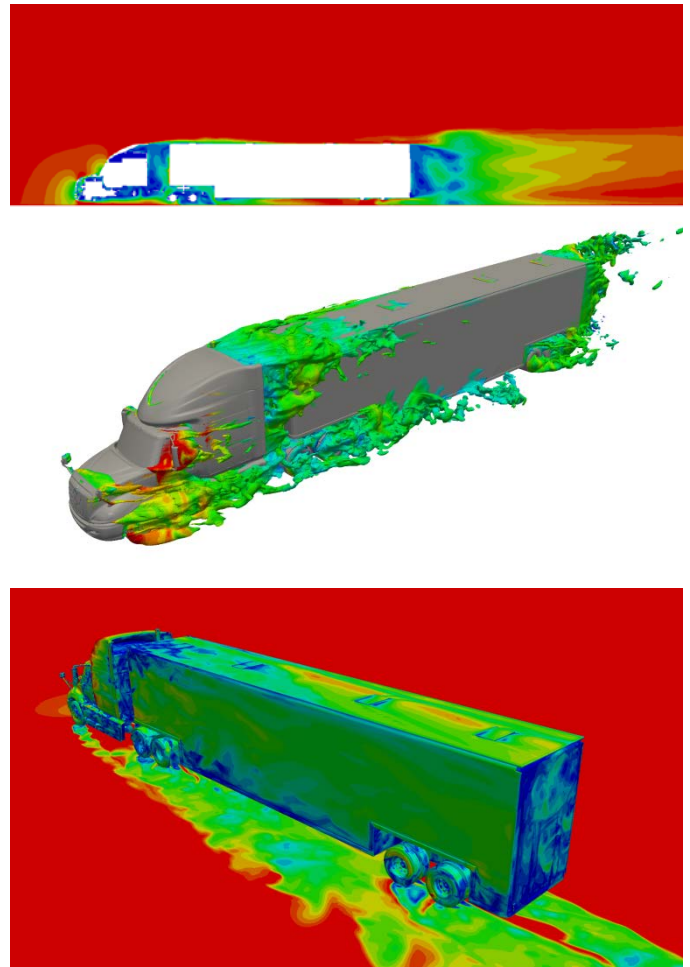


Figure 5. Examples of standard post-processing output.

## Validation Process

The validation process for the CFD software has involved extensive testing at a variety of aerodynamic facilities around the world. These have comprised both model-scale and full-scale aerodynamic wind tunnels, with fixed floor and moving ground.

All of the tests have been conducted by Streamline Solutions except for the 'DRIVAER' models which come from work conducted by Technische Universität München, presented at the 2012 SAE World Congress [6].

Well over 100 different configurations have been compared between CFD and experiment, covering a wide variety of vehicle shapes:

- Sedan
- Hatchback
- Estate
- SUV
- Sportscar
- Streamliner
- NASCAR
- Indycar

- Light duty truck
- Heavy duty truck (articulated, or 'semi' trucks)



Figure 6. Example vehicle test items.

They have also covered a range of experimental conditions:

- Fixed ground
- 5-belt moving ground
- Single belt moving ground
- Yaw angle
- Ride height
- Test speed
- Vehicle cooling configuration (open, closed, etc.)



Figure 7. Full-scale test facilities used.

Figure 7 illustrates that a significant proportion (over a third) of the validation cases were compared to full-scale tunnels around the world, including:

- FKFS Vehicle Aero-Acoustics Wind Tunnel [7] [8]
- Volvo Cars PVT Wind Tunnel [9]
- Chrysler Aero-Acoustics Wind Tunnel [10]
- Windshear Wind Tunnel [11]
- Ford DTF Wind Tunnel No.8 [12]
- Ford Cologne Wind Tunnel [13]

The majority of the rest of the validation data came from the Auto Research Center model-scale wind tunnel in Indianapolis. The ARC facility is a Gottingen type tunnel with an open test section, a single belt rolling road system and temperature control. The model scales vary from 1/8th scale for semi-trucks to 50% scale for open-wheel motorsport applications.

Table 1. ARC wind tunnel specifications.

Max Wind Speed	50 m/s	Boundary Layer Thickness	1 mm
Max Road Speed	50 m/s	Primary BL Motor Power	80 kW
Nozzle Size	2.3 m x 2.1 m	Secondary BL Motor Power	19 kW
Contraction Ratio	4.8 : 1.0	Rolling Road Motor Power	120 kW
Moving Belt Size	3.4 m x 1.7 m	Main Fan Motor Power	320 kW

Figure 8 shows the layout of the tunnel and related facilities.

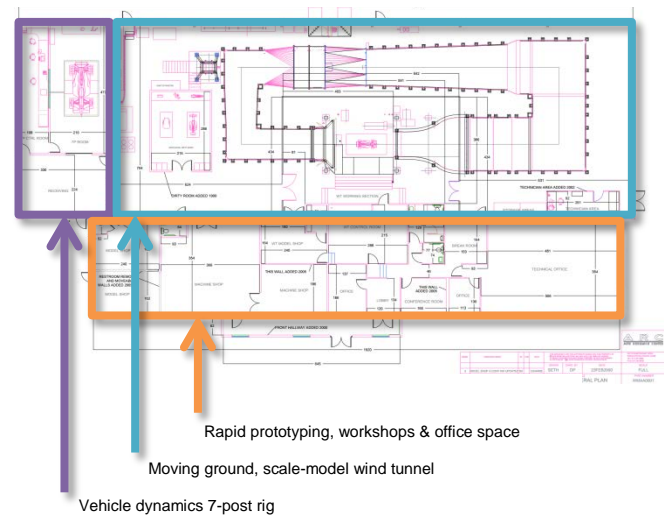


Figure 8. ARC wind tunnel layout.

The models are mounted in the tunnel by means of an overhead sting. The 6-component aerodynamic balance is contained within the model and is tightly integrated with a proprietary model motion system that allows for automatic yaw, pitch, roll, heave and steer during a wind tunnel run. The model motion system is linked with two lasers on-board the vehicle for closed loop control of vehicle ride height.

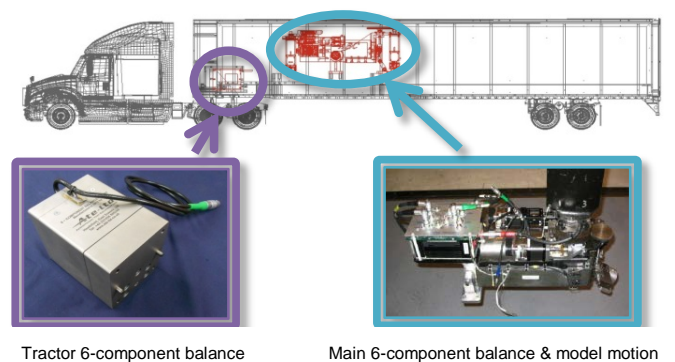


Figure 9. Dual balance set-up for semi-truck testing.

Figure 9 shows the internal balance arrangement for a semi-truck test. In this case the tractor forces and moments are separated out from the trailer's through the use of a secondary balance located at the fifth wheel. Similar secondary balances are also used in motorsport to directly measure the contribution of the front and rear wings.

In addition to the 6-component balances, the tunnel also has 128 pressure channels to allow for evaluation of surface pressures from around the model. For cooling airflow measurement a grid of up to 14 vane anemometers can be used to not only evaluate total mass-flow but also to provide insight into the flow distribution across any heat exchangers.

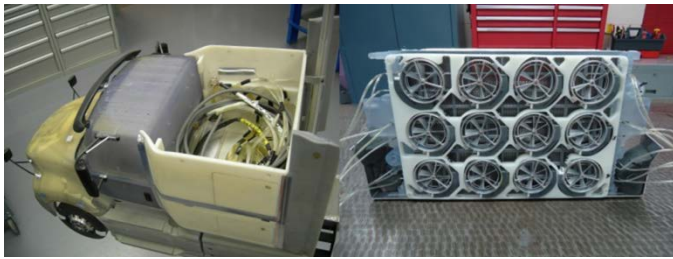


Figure 10. Pressure measurement and vane anemometers.

## Results

A small subset of the results is presented in the tables below, commercial confidentiality prevents us from presenting much of the data we have accumulated. All of the tests have been conducted by Streamline Solutions except for vehicle numbers 1,2 and 3 which were conducted by Technische Universität München [6].

Table 2. Validation results matrix.

Vehicle No.	Vehicle Model	Grille (open, closed, blanked)	Wind Tunnel Data		Elements		
			Scale	Ground Simulation	Coefficients		
					CD	CLF	CLR
1	DRIVAER Estate	n/a	40%	Single Belt	2.40%		
2	DRIVAER Fast	n/a	40%	Single Belt	-0.41%		
3	DRIVAER Notch	n/a	40%	Single Belt	0.41%		
4	Sedan 1	open	100%	5 Belt	0.67%	-0.67%	-6.56%
		open	40%	Single Belt	0.00%	-7.19%	4.45%
		closed	40%	Single Belt	1.74%	-2.48%	4.61%
5	Sedan 2	open	100%	5 Belt	0.00%	-1.87%	-0.37%
		blanked	100%	Fixed	1.57%	-26.38%	9.84%
6	Sedan 3	closed	100%	Fixed	2.35%		
		open	40%	Single Belt	0.32%	-2.27%	-2.27%
		closed	40%	Single Belt	2.03%	-1.35%	2.03%
7	Estate 1	open	40%	Single Belt	-0.32%	11.04%	26.62%
8	Estate 2	open	100%	5 Belt	-0.95%	-3.81%	-3.17%
9	Hatchback 1	open	40%	Single Belt	3.09%	7.21%	19.75%
10	Hatchback 2	open	100%	5 Belt	2.18%	-22.55%	12.00%
11	SUV 1	open	40%	Single Belt	0.81%	6.59%	-16.76%
12	NASCAR 1		40%	Single Belt	2.22%		
13	NASCAR 2	open	40%	Single Belt	-1.25%	-32.67%	-10.47%
14	Semi-Truck 1	open	12.5%	Single Belt	0.19%		
15	Light Truck 1	open	20%	Single Belt	-0.38%	-5.09%	-10.38%

Average Error Magnitude 1.2% 9.37% 9.24%

For case 14, which utilized the dual balance set-up, the tractor drag was predicted to an error magnitude of 1.8%, whilst the trailer drag had an error magnitude of 3.4%.

Table 3. Truck specific validation cases.

Vehicle No.	Vehicle Model	Grille (open, closed, blanked)	Yaw	Wind Tunnel Data		Elements		
				Scale	Ground Simulation	Coefficients		
						CD	CLF	CLR
21	Semi-Truck 2	open	0.000	0.125	Single Belt	0.19%		
		open	0.000	0.125	Single Belt	-1.13%		
		open	6.000	0.125	Single Belt	2.63%		
		open	6.000	0.125	Single Belt	3.45%		
		open	6.000	0.125	Single Belt	3.45%		
		open	0.000	0.125	Single Belt	2.25%		
		open	-6.000	0.125	Single Belt	4.85%		
		open	9.000	0.125	Single Belt	2.50%		
		open	-9.000	0.125	Single Belt	3.13%		
		open	9.000	0.125	Single Belt	0.00%		
		open	9.000	0.125	Single Belt	2.06%		
		22	Light Truck 2	open	0.000	0.125	Single Belt	-0.38%
open	6.000			0.125	Single Belt	2.69%	-0.36%	-17.95%
open	3.000			0.125	Single Belt	1.47%	-3.87%	14.73%
23	Semi-Truck 3	open	0.000	0.125	Single Belt	0.57%		
		open	3.000	0.125	Single Belt	4.13%		
		open	6.000	0.125	Single Belt	4.98%		
24	Semi-Truck 4	open	0.000	0.125	Single Belt	1.11%		

Average Error Magnitude 2.5% 3.11% 14.35%

The result of the more than one hundred different test cases is a best practice that consistently delivers drag coefficient error magnitudes less than 2% for passenger cars, and 4% for heavy trucks. The average lift error magnitudes, for both front and rear axle coefficients, are less than 10%.

In addition to the excellent correlation achieved the transient run times are also extremely competitive. With typical mesh sizes of 50-80 million cells running on 144 cores (32GB ram nodes with dual Intel Six Core Xeon E5-2640 2.5GHz with QDR Infiniband interconnect), turnarounds of 16-24 hours are normal. That includes 2-3 hours meshing time and a few minutes for the automated post-processing.

Although the error magnitudes already meet targets in more than 80% of cases (with the mean error significantly less than target) further work is still progressing to make improvements. We have found that square back vehicles (such as estate and hatch backs, and trucks) are more sensitive to time-step size than sedan shape vehicles.

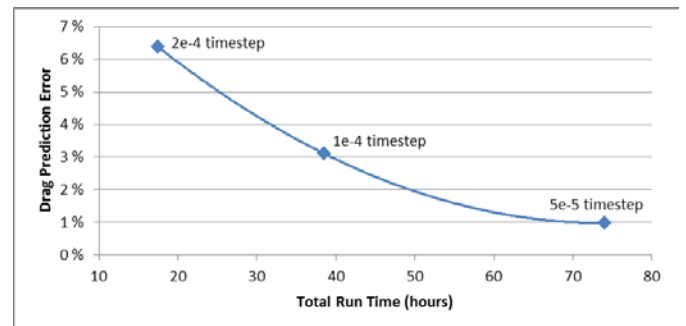


Figure 11. Drag prediction error vs. total run time for a semi-truck.

Figure 11 shows that the user has the flexibility to choose the compromise between turnaround time and accuracy. As an example, for large Design Of Experiment (DOE) style optimizations a half-car approach, with larger time steps, offers run times that are only 15% of the full-vehicle best practice approach (2.5-3.5 hours on 144 cores).

Finally, the results presented were calculated with a rotating wall boundary condition, and whilst accurate enough for overall aerodynamic forces further work is on-going to implement a sliding mesh approach to better capture the flow field around the wheels and tires. Currently this doubles run times, however development is progressing to reduce this deficit.

### Flowfield Comparison

In addition to the integral forces presented above extensive work was conducted to compare the flow field and more specifically the surface pressure distributions. The figures below illustrate the correlation between the CFD predictions and wind tunnel data for the DrivAer models.



Figure 12. The DrivAer model in the Technische Universität München wind tunnel A .

Figures 13 and 14 show comparisons of the upper and lower centerline section pressure distributions for the fastback model.

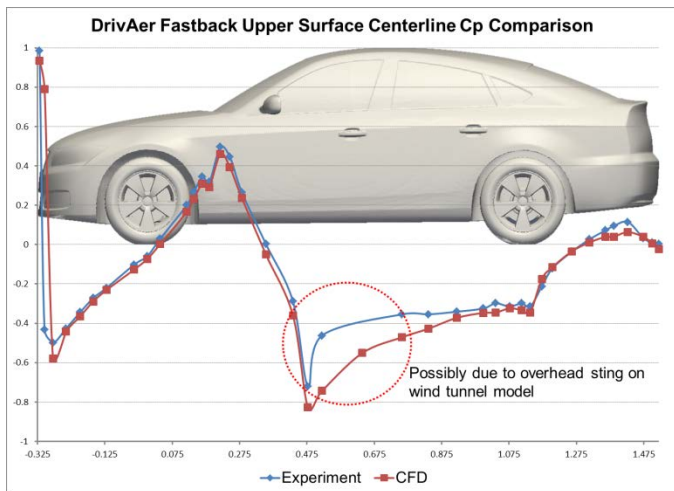


Figure 13. DrivAer fastback upper surface centerline Cp comparison.

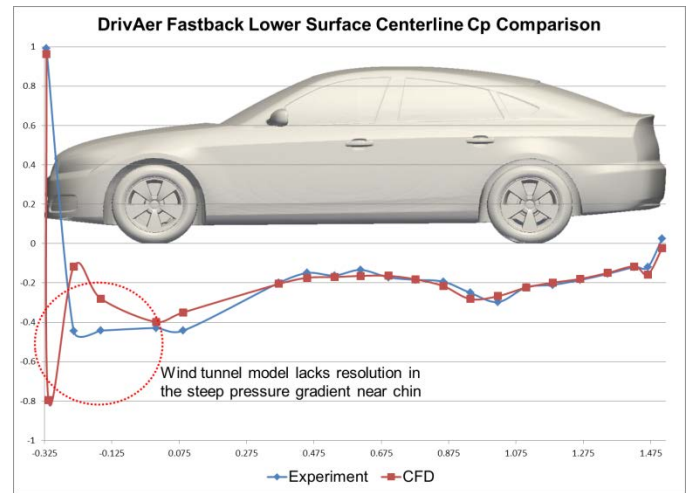


Figure 14. DrivAer fastback lower surface centerline Cp comparison.

Figure 13 shows a difference near the leading edge of the roof that is probably due to the sting present in the wind tunnel (see Figure 12). Figure 14 shows some differences near the chin that are due to a lack of resolution in the wind tunnel pressure tapping scheme (there are only 2 taps in front of the front axle).

Figures 15 through 19 show a subjective comparison of surface pressure distribution on the windshield, side-glass and rear screen of the DrivAer models.

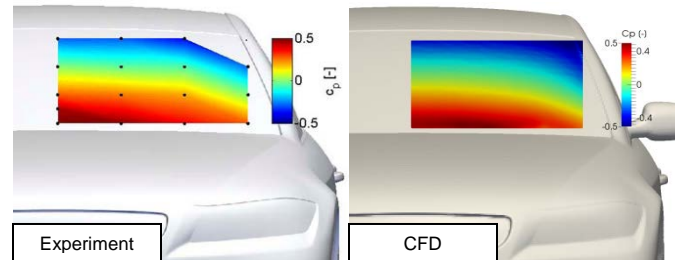


Figure 15. DrivAer fastback windshield Cp comparison.

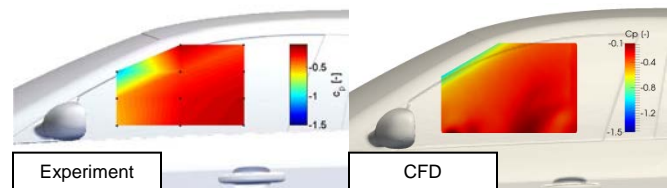


Figure 16. DrivAer fastback side-glass Cp comparison.

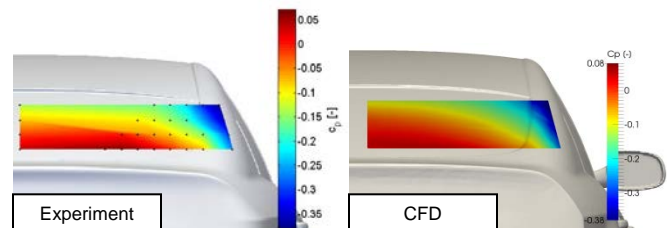


Figure 17. DrivAer fastback rear screen Cp comparison.



Figure 18. DrivAer notchback rear screen Cp comparison.

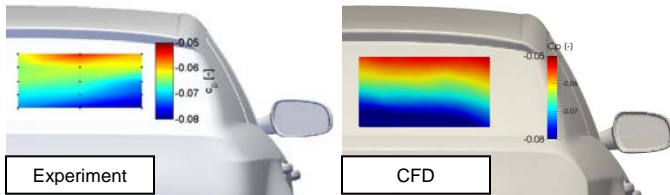


Figure 19. DrivAer estateback rear screen Cp comparison.

There is a small discrepancy at the top of the A-pillar on Figure 16, which may be due to the pressure tap recording total pressure rather than static (as it is very close to a vortex core). The discrepancy in pattern on the estate back needs to take into account the very small Cp range that is covered.

## Summary/Conclusions

The result of this project is a set of best practices that consistently delivers drag coefficient error magnitudes less than 2% for passenger cars, and 4% for heavy trucks.

The CFD results have been heavily validated in a range of wind tunnels, and for a variety of different vehicle shapes.

For typical mesh sizes of 50-80 million cells, running on 144 cores, turnarounds of 16-24 hours are the median. This is considered to be extremely competitive when compared to other commercial CFD codes.

## Future Work

Although the accuracy already meets targets in more than 80% of cases (with the mean error significantly less than target) further work is still progressing to make improvements. Some areas that are currently being addressed are:

- Wheels and fans: sliding mesh for rotating objects
- Hybrid convection schemes for RANS/LES
- DES model improvements
- Time step and schemes
- Coupled solvers
- Adjoint solver

## References

1. "Guidelines for Aerodynamic Assessment of Medium and Heavy Commercial Ground Vehicles Using Computational Fluid Dynamics," SAE Standard J2966\_201309, 2013,
2. P. Spalart, W. Jou, M Strelets, and S. Allmaras, "Comments on the feasibility of les for wings, and on a

hybrid rans/les approach," In Advances in DNS/LES, pages 137–147, Proceedings of the First AFSOR International Conference on DNS/LES, 1997.

3. E. de Villiers, "The Potential of Large Eddy Simulation for the Modeling of Wall Bounded Flows," PhD thesis, Imperial College, London, UK, 2006.
4. M. Islam, F. Decker, E. de Villiers et al., "Application of Detached–Eddy Simulation for Automotive Aerodynamics Development," SAE 2009-01-0333, 2009
5. P.R. Spalart, S. Deck, M. Shur, K Squires, M. Strelets, and A. Travin, "A new version of DES resistant to ambiguous grid densities," Theoretical and Computational Fluid Dynamics, 20:181–195, 2006.
6. A. I. Heft, T. Indinger, N. A. Adams, "Introduction of a New Realistic Generic Car Model for Aerodynamic Investigations," SAE 2012 World Congress, April 23-26, 2012, Detroit, Michigan, USA, Paper 2012-01-1068
7. Künstner, R., Potthoff, J., and Essers, U., "The Aero-Acoustic Wind Tunnel of Stuttgart University," SAE Technical Paper 950625, 1995, doi:10.4271/950625.
8. Wiedemann, J., "The Influence of Ground Simulation and Wheel Rotation on Aerodynamic Drag Optimization - Potential for Reducing Fuel Consumption," SAE Technical Paper 960672, 1996, doi:10.4271/960672.
9. Sternéus, J., Walker, T., and Bender, T., "Upgrade of the Volvo Cars Aerodynamic Wind Tunnel," SAE Technical Paper 2007-01-1043, 2007, doi:10.4271/2007-01-1043.
10. Walter, J., Duell, E., Martindale, B., Arnette, S. et al., "The DaimlerChrysler Full-Scale Aeroacoustic Wind Tunnel," SAE Technical Paper 2003-01-0426, 2003, doi:10.4271/2003-01-0426.
11. Walter, J., Bordner, J., Nelson, B., and Boram, A., "The Windshear Rolling Road Wind Tunnel," SAE Int. J. Passeng. Cars - Mech. Syst. 5(1):289-303, 2012, doi:10.4271/2012-01-0300.
12. Walter, J., Duell, E., Martindale, B., Arnette, S. et al., "The Driveability Test Facility Wind Tunnel No. 8," SAE Technical Paper 2002-01-0252, 2002, doi:10.4271/2002-01-0252.
13. Volkert, R. and Kohl, W., "The New Ford Aerodynamic Windtunnel in Europe," SAE Technical Paper 870248, 1987, doi:10.4271/870248.

## Contact Information

Auto Research Center  
 4012 Championship Drive  
 Indianapolis, IN 46268  
 Tel: +1.317.291.8600  
 Fax: +1.317.291.8700  
 Email: sales@arcindy.com  
 Web: [www.arcindy.com](http://www.arcindy.com)

## Acknowledgments

I would like to acknowledge the help and support of my co-authors, but also all the other employees at the Auto Research Center, Engys and Streamline Solutions who have contributed to the development of Elements, as well as the extensive wind tunnel data used to validate it.